Lab on a Chip

COMMUNICATION

View Article Online
View Journal | View Issue

Cite this: *Lab Chip*, 2015, **15**, 43

Received 17th June 2014,
Accepted 16th October 2014

DOI: 10.1039/c4lc00704b

www.rsc.org/loc

Microscale anechoic architecture: acoustic diffusers for ultra low power microparticle separation *via* traveling surface acoustic waves

Jan Behrens,[ab] Sean Langelier,[c] Amgad R. Rezk,[a] Gerhard Lindner,[b] Leslie Y. Yeo*[a] and James R. Friend*[ad]

We present a versatile and very low-power traveling SAW microfluidic sorting device able to displace and separate particles of different diameter in aqueous suspension; the travelling wave propagates through the fluid bulk and diffuses *via* a Schröder diffuser, adapted from its typical use in concert hall acoustics to be the smallest such diffuser to be suitable for microfluidics. The effective operating power range is two to three orders of magnitude less than current SAW devices, uniquely eliminating the need for amplifiers, and by using traveling waves to impart forces directly upon suspended microparticles, they can be separated by size.

Most lab-on-a-chip devices are employed for biological or medical applications, requiring some means of cell or particle manipulation.[1] Investigators have explored hydrodynamic,[2] dielectrophoretic,[3] optical,[4] magnetic,[5] and acoustic forces[6,7] to control particle and colloid behaviour, with modest success so far. Standing surface acoustic waves (SSAW) have become remarkably popular, driving particles toward vibration nodes laterally distributed across a channel.[8–10]

The typical SSAW arrangement employs two interdigital transducers (IDTs) with a microchannel set between them; the width of the channel is typically restricted to allow only one vibration node down its midplane and parallel to its walls.[9] All devices constructed to use SSAW have a plane of symmetry down the middle of the microfluidic channel, reducing by half the effective length of actuation across the channel. Larger particles, or those particles possessing a positive contrast factor (ϕ; dependent upon the particle density and its compressibility in comparison to the surrounding medium) move more quickly to a node of vibration upon exposure to the acoustic radiation while particles with negative contrast factor migrate to the antinodes.[11] Splitting the outflow of the channel allows the particles to be separated and collected.

An alternative is *traveling* surface acoustic waves (TSAW)—the wave travels without reflection across the channel—utilizing the entire channel without a plane of symmetry down its middle. Published reports of such devices are, however, few in number; the first known made use of a trapezoidal cross-sectioned microchannel[12] with SAW propagating with a slight angle with respect to the channel's long axis to drive fluid flow in the channel and simultaneously steer particles laterally. However, this arrangement contained an open microchannel without continuous particle separation, and fabricating oddly sloped walls in a microchannel in lithium niobate is tedious.

These issues were subsequently addressed to some extent by Johansson *et al.*,[13] and rather more elegantly by Destgeer *et al.*, through matching the width of a traditional square channel to the attenuation length of the sound propagating in the fluid,[14]† while simultaneously ensuring that the frequency chosen for the SAW is high enough to cause its rapid and complete absorption by the fluid in the channel, therefore ensuring the incident SAW is indeed traveling. In their study, 100 mW-order acoustic radiation was used to drive particle deflection, but also was responsible for acoustic streaming that may upset the particle trajectories, streaming that was obvious from the presence of single flow vortices across the width of the channel. Unfortunately, standing waves are very easily generated in fluid volumes, even when confined using material with a nearly identical acoustic impedance, for example, water as bounded by polydimethylsiloxane (PDMS).[15,16] Thus, even weak standing waves can overwhelm traveling waves in the manipulation of particles.

If pure traveling waves could be generated, particle positioning could be controlled based upon the time of exposure because the force upon a particle due to a traveling acoustic wave will be constant over the entire width of the channel, unlike SSAW-based particle forces which vary depending

[a] *Micro/Nanophysics Research Laboratory, RMIT University, Melbourne, VIC 3000, Australia. E-mail: jfriend@eng.ucsd.edu, leslie.yeo@rmit.edu.au*
[b] *Institute of Sensor and Actuator Technology, Coburg University of Applied Sciences and Arts, Coburg 96450, Germany*
[c] *Melbourne Centre for Nanofabrication, Clayton, VIC 3800, Australia*
[d] *Department of Mechanical and Aerospace Engineering, University of California-San Diego, 9500 Gilman Dr, San Diego CA 92093, USA*

upon how far the particle is from a node. It is important to remember that the attenuation length of sound in fluid is typically tens of centimeters, far longer than the attenuation length of SAW in a lithium niobate substrate exposed to such a fluid,[17] and so the channel for a TSAW device can potentially be very wide if needed. Likewise, if a means could be identified to remove the limitation of tying the SAW frequency to the channel width as with Destgeer, *et al.*, then the channel width could be made very narrow as well, far more narrow than the attenuation length of sound in the fluid. This would provide flexibility in designing flow focusing and improved mass flow as needed. By introducing SAW perpendicular to the flow direction of the channel, the particles can be driven laterally across the channel while exposed to the SAW.

In this letter, we borrow a simple tool of concert hall acoustics—the *Schröder diffuser*—to generate TSAW through diffusion of reflections from the wall of the microfluidic channel farthest from the source of acoustic radiation. We demonstrate that in doing so, the power required to separate microparticles is two orders of magnitude lower than what is required in SSAW and acoustic streaming devices reported to date, a very low power alternative (0.75 mW) that greatly simplifies the driver circuitry required, and provides substantial flexibility in the choice of channel dimensions for microparticle separation in a continuous flow configuration.

Concert halls and similar architecture require carefully engineered surfaces to provide evenly distributed acoustic energy free of direct echoes. These surfaces either absorb the incoming sound or diffuse it, and diffusion is preferred because no sound energy is lost. The key feature of such diffusers is the absence of sound returning along the incident path which would otherwise form standing waves: exactly what we desire in our microdevice. In the 1970s, Schröder introduced a novel diffuser[18] which came to bear his name and offered optimal sound diffusion over a specific frequency range with only a few simple design equations that are solvable using the quadratic residue (QR) method: $w = \lambda_{min}/2 - T$, $s_i = i^2 \bmod N$, and $\lambda_i = s_i\lambda_0/(2N)$. The ith slot, $i \in \{1,\ldots,N\}$, of all N slots per acoustic period forms the diffuser, with w, λ_i, and T as the slot width, depth of the ith slot, and the dividing fin width, respectively. The wavelengths λ_{min} and λ_0 refer to the minimum and maximum (or design) wavelengths that form the range of operation for the diffuser. Here we have reduced the diffuser's scale from the 10^{-1}–10^{0} m order typical of concert halls to 10^{-5} m for dealing with the 10^{7}–10^{8} Hz acoustic waves in the fluid due to the SAW, as illustrated in Fig. 1‡ : architecture on the microscale to diffuse sound from the fluidic channel and form TSAW.

A Schröder diffuser (N = 37) was fabricated in Si (see Fig. 1(a)–(c)) as an integral part of a fluid separation channel, opposite an interdigital transducer (IDT) deposited on a lithium niobate substrate, and with inlet and outlet channels as shown in Fig. 1(a, d). Set onto a channel of 3 mm width and 60 μm depth, the diffuser was designed to operate using water (bulk sound speed c = 1482 m s^{-1}) from

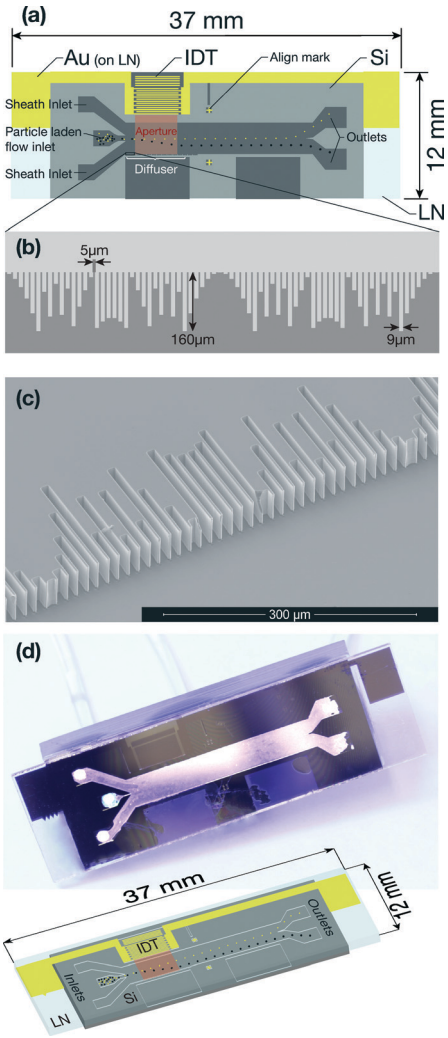

Fig. 1 (a) The device illustrated through the bottom of the transparent LN; the Au electrode is atop the LN and the Si layer with etched channel and diffuser features is bonded to the LN's top surface. Opposite the interdigital transducer (IDT), the diffuser diffuses the incident acoustic radiation in the fluid from leakage of the SAW generated by the IDT. (b) The Schröder diffuser design has cavities of different depths (c) present in the Si along the channel in a scanning electron microscope image. (d) A photograph and matching device diagram shows the 1.45 mm wide sheath flow inlets aside the centrally aligned, 100 μm-wide particle channel, the 3 mm wide main channel, and 1.5 mm wide outlets. Note the PDMS structure and hoses atop the Si for fluid connection.

$f_0 = c/\lambda_0$ = 5 MHz to $f_{max} = c/\lambda_{min}$ = 50 MHz. A single, 30 MHz SAW IDT was fabricated on a lithium niobate (LN, 127.86° *Y*-rotated, *X*-propagating single crystal $LiNbO_3$, Roditi Ltd., London, UK) substrate with an aperture of 4 mm and 19 finger pairs, in a simple unweighted configuration and on one side of the channel. Standard alignment was performed to bond the Si and LN together using UV epoxy bonding previously reported.[15] The IDT has an external reflector near the edge of the device to suppress triple transit echoes. Using Si has the advantage here of having a much different acoustic impedance than water: if the

diffuser works in this configuration, it should work with most other material combinations. In fact, producing the channel and diffuser structure in PDMS produces results identical to the LN and Si configuration.

Fluorescent polystyrene particles 4.5, 25, and 45 μm in diameter (Polysciences, Warrington PA, USA) were pumped through the device using a syringe pump (NE–1002, New Era Pump Systems, Farmingdale, NY USA) at a flow rate of 400 μl h^{-1} *via* the 100 μm wide channel set between two 1.45 mm wide channels that provide sheath flow at 1500 μl h^{-1}, forming a linear flow velocity profile at approximately 2.3 mm s^{-1} across the channel width. The SAW operated at 250 μW to 3 mW to assess particle translation and separation. The SAW was driven with only a signal generator (N9310A, Agilent, Santa Clara, USA), monitored *via* an oscilloscope (RTO1044, Rhode & Schwarz, Munich, Germany) with appropriate current and voltage probes. This is the only acoustic microfluidics device able to function without an amplifier to the authors' knowledge.

The particles flowing along the channel consistently translate *away* from the acoustic source's aperture (see Fig. 1(a)). The 2 mW SAW acoustic radiation has a substantial influence only upon larger, 45 μm particles (conc. of 10 particles μl^{-1}) amid 4.5 μm particles (conc. of 2000 μl^{-1}). Both 25 μm and 45 μm particles (both at 10 particles μl^{-1}) were translated upon exposure to 2 mW SAW as shown in Fig. 2(b); the 45 μm particles exhibit nearly 1.5 mm of translation over the 4 mm aperture.

Closer examination of the 25 μm and 45 μm particles' lateral velocity from Fig. 2(b) while exposed to TSAW over the IDT aperture A (Fig. 2(c)), suggests a linear relationship between the particle translation velocity and the input power. Generally, the particles are uniformly driven across the width of the channel by from 0.25 mW to 2.5 mW of acoustic radiation: the coefficient of determination, R^2, of the particle translation velocity is at or above 0.7 in Fig. 2(d) over this range. At higher power, off-axis, diffuse acoustic waves result in the formation of weak, spurious standing waves across the channel width, leading to non-uniform particle translation, a growing standard deviation in the translation velocity and a rapid reduction in R^2. The plotted values were determined using ImageJ and the Mosaic plug-in (National Institutes of Health, Washington D.C. USA) on experiment videos (D600, Nikon, Shinjuku Japan and K2–SC, Infinity, Boulder, CO USA).

We compare our measurements to King's[19] theoretical estimate of the acoustic radiation force on a particle during exposure to the TSAW. The observations in Fig. 2(a) are qualitatively consistent with King's results which note that "large" particles experience significantly larger forces from acoustic radiation than "small" ones.[19]§ During exposure to the 30 MHz TSAW, the "small" 4.5 μm particles did not exhibit a visible deflection, while the "large" 45 μm particles translated approximately 1.5 mm over a 4 mm run. Because we are using 10 MHz-order acoustic waves with particles of size 10 μm and larger, the many simplifications from his

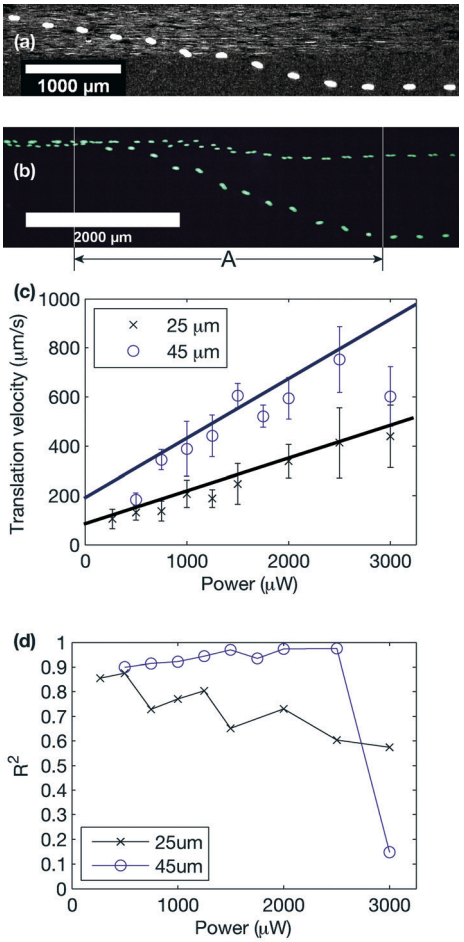

Fig. 2 (a) Particles 45 μm in diameter were found to be displaced as they transit through the 4 mm long diffuser region and aperture a while coflowing 4.5 μm particles were left unaffected: the direct acoustic force was significant only upon the larger particles at 30 MHz. (b) The displacement is dependent upon the particle size, shown with 25 μm and 45 μm particles across (c) a large range (0.25 to 3 mW) of SAW input power (error bars are standard deviation over three separate runs). Acoustic forces on the particles (see text) according to theory are (c) plotted with solid lines that correlate well with the measurements, and (d) the coefficient of determination, R^2, of the particle translation velocity with respect to input power shows uniform translation over 0.25 to 2.5 mW.

"small" size assumption that result in the well-known, concise *King's equation* are inappropriate: we must use the full form for the radiation force F_R on the individual particles as follows:[19]

$$F_R = 2\pi\rho_0 \frac{A^2}{\alpha^2}\left[\frac{1}{LM} + \frac{2(\alpha^2 - 3(1-\rho_0/\rho_p))^2}{MN\alpha^8}\right],$$
$$L = \frac{1}{\alpha^2}(1+\alpha^2),\ N = \frac{81}{\alpha^{10}}\left[1 + \frac{1}{9}\alpha^2 - \frac{2}{81}\alpha^4 + \frac{1}{81}\alpha^6\right], \quad (1)$$
$$M = \frac{4}{\alpha^6}\left[\left(1 + \frac{\rho_0}{2\rho_p}\right)^2 + \frac{1}{2}\alpha^2\left(1 + \frac{\rho_0}{2\rho_p}\right)\frac{\rho_0}{\rho_p} + \frac{1}{4}\alpha^4\right].$$

The radiation force (F_R) on the particle is balanced by the drag force, $F_{drag} = 6\pi\mu ua$, the latter restraining the particle's lateral motion across the channel; μ and u are the fluid viscosity and particle velocity. It can be seen that good quantitative agreement was obtained between theory and experiment in Fig. 2(c).

Input power appears to be a linear function of the displacement velocity over the range of power considered. Consistent with these experimental observations, King's equation predicts $F_R \sim P$ where P is the input SAW power, since $F_R = A^2$, $A \sim u_{SAW}$, and $u_{SAW}^2 \sim P$. Below 0.5 mW the particles were displaced but did not separate; above 2.75 mW, the diffused acoustic radiation interfered with the incident acoustic wave from the SAW, forming a weak standing wave across the channel width of sufficient strength to affect the particle motion, resulting in a stepwise translation of the particles across the width of the channel and away from the IDT with a spacing of $\lambda/2$. The error bars, representing the standard deviation in the displacement velocity in the IDT aperture over at least three runs, are much larger at 3 mW as a consequence, and the coefficient of determination R^2 of the particle traces decreases (Fig. 2(d)). By using a higher frequency of 50 MHz, it was possible to move the 25 μm particle over distances similar to what was achieved with 45 μm particles driven at 30 MHz: the particles were propelled into the channel wall opposite the SAW IDT. By increasing the frequency further with judicious design of the diffuser per the design rules espoused by Schröder, the transport of even smaller particles should be possible.

Practically, there is an upper limit to the diffuser's operating frequency due to fabrication limitations; in routine UV photolithography it is 1 μm. Taking this value as the slot width, w, then the wavelength $\lambda_{min} = 2$ μm giving $f_{max} = c/\lambda_{min} = 2$ GHz as the upper limit. Beyond a frequency of about 500 MHz, the viscosity of the fluid is effective at easily absorbing the SAW and thus preventing reflections over length scales commensurate with microfluidics,[20] but this comes at the cost of generating acoustic streaming that interferes with the bulk flow. Though we report results using Si and UV epoxy bonding, we have likewise used convenient PDMS casting and bonding techniques.

In summary, we have presented a versatile and exceptionally low-power, traveling wave SAW microfluidics device that can displace and separate particles of different diameter; the travelling wave propagates through the fluid bulk and diffuses upon the Schröder diffuser designed for this application. The effective operating power range is two to three orders of magnitude less than required in SSAW devices, and by using traveling waves, forces can be imparted upon a particle across the width of the channel to effectively transport it.

References

† Friend, Destgeer, and Jung at Flow '14, University of Twente, 20 May 2014, discussed the choice of SAW frequency to ensure the attenuation length of sound in the fluid was approximately the same as the width of the channel, and the limitation in selection of the channel's width to a value defined by the frequency of the acoustic radiation.

‡ The authors thank Philipp Gutruf and Andreas Bös for their help in preparing the results for this figure.

§ King's "small" particle size assumption is written as $\alpha \equiv ka \ll 1$, where $k = 2\pi/\lambda$ is the wavenumber, λ is the sound wavelength in the fluid, and a is the microparticle radius.

1 J. Nilsson, M. Evander, B. Hammarström and T. Laurell, *Anal. Chim. Acta*, 2009, **649**, 141–157.
2 A. Karimi, S. Yazdi and A. M. Ardekani, *Biomicrofluidics*, 2013, **7**, 021501.
3 R. Pethig, *Biomicrofluidics*, 2010, **4**, 022811.
4 K. Dholakia and T. Čižmár, *Nat. Photonics*, 2011, **5**, 335–342.
5 C. Liu, T. Stakenborg, S. Peeters and L. Lagae, *J. Appl. Phys.*, 2009, **105**, 102014.
6 H. Mulvana, S. Cochran and M. Hill, *Adv. Drug Delivery Rev.*, 2013, **65**, 1600–1610.
7 Z. Wang and J. Zhe, *Lab Chip*, 2011, **11**, 1280–1285.
8 M. K. Tan, J. R. Friend and L. Y. Yeo, *Lab Chip*, 2007, **7**, 618–625.
9 J. Shi, H. Huang, Z. Stratton, Y. Huang and T. J. Huang, *Lab Chip*, 2009, **9**, 3354–3359.
10 S.-C. S. Lin, X. Mao and T. J. Huang, *Lab Chip*, 2012, **12**, 2766–2770.
11 H. Bruus, *Lab Chip*, 2012, **12**, 1014–1021.
12 M. K. Tan, R. Tjeung, H. Ervin, L. Y. Yeo and J. Friend, *Appl. Phys. Lett.*, 2009, **95**, 134101.
13 L. Johansson, J. Enlund, S. Johansson, I. Katardjiev, M. Wiklund and V. Yantchev, *J. Micromech. Microeng.*, 2012, **22**, 025018.
14 G. Destgeer, K. H. Lee, J. H. Jung, A. Alazzam and H. J. Sung, *Lab Chip*, 2013, **13**, 4210–4216.
15 S. Langelier, L. Yeo and J. R. Friend, *Lab Chip*, 2012, **12**, 2970–2976.
16 I. Leibacher, S. Schatzer and J. Dual, *Lab Chip*, 2014, **14**, 463–470.
17 M. B. Dentry, L. Y. Yeo and J. R. Friend, *Phys. Rev. E: Stat., Nonlinear, Soft Matter Phys.*, 2014, **89**, 013203.
18 M. R. Schröder, *J. Acoust. Soc. Am.*, 1975, **57**, 149–150.
19 L. V. King, *Proc. R. Soc. London, Ser. A*, 1934, **147**, 212–240.
20 M. B. Dentry, L. Y. Yeo and J. R. Friend, *Phys. Rev. E: Stat., Nonlinear, Soft Matter Phys.*, 2014, **89**, 013203.

